Direct part density inspection in laser powder bed fusion using eddy current testing

Joint Special Interest Group meeting between euspen and ASPE
Advancing Precision in Additive Manufacturing
Inspire AG, St. Gallen, Switzerland 2021
www.euspen.eu

Direct part density inspection in laser powder bed fusion using eddy current testing

Adriaan B. Spierings[1], Marvin A. Spurek[1,2], Marc Lany[3], Gilles Santi[3], Bernard Revaz[3], Konrad Wegener[2]

[1]inspire AG, Innovation Center for Additive Manufacturing (icams), CH-9014 St.Gallen, Fürstenlandstrasse 122, Switzerland
[2]Swiss Federal Institute of Technology, ETH Zurich, Institute of Machine Tools and Manufacturing, CH-8092 Zurich, Leonhardstrasse 21, Switzerland
[3]Sensima Inspection SARL, 1196 Gland, 2 Route Cite Ouest, Switzerland

spierings@inspire.ethz.ch

Abstract
The direct qualification of additively manufactured (AM) metal components fabricated by laser powder bed fusion (LPBF), or the certification of the corresponding AM processes, remains a challenge due to the many influencing parameters, and process-inherent variability. Hence, components lack consistent quality regarding dimensional accuracy, surface quality, and material integrity, since internal defects such as pores and cracks are typical characteristics of such components. Different sensing technologies such as melt-pool monitoring are considered for in-process material integrity assessment, and for process control. However, although melt-pool monitoring provides process related information on the laser-material interaction such as melt-pool temperature and size, it does only indirectly provide sufficient information on the quality and integrity of the layer-wise generated material. Eddy current testing (ECT) is a well-established NDT technique for part quality inspection in many industries, and specifically suited to detect near-surface material defects such as e.g. cracks. This characteristic makes ECT a promising monitoring technology for the layer-wise monitoring of material quality in AM processes. Its integration into a LPBF-machine allows to generate direct material integrity data while the layer-wise acquisition offers potentials to monitor the individual part quality over a full build process, minimizing thereby post-process quality assessment measures. The basic feasibility of an ECT system to directly measure part density demonstrated, using LPBF processed SS316L samples with different densities.

Laser powder bed fusion, Eddy Current, part integrity monitoring

1. Introduction

Additive manufacturing (AM) technologies offer industrially relevant advantages for the tool-less production of highly complex parts directly from CAD data. Thereby, Metal Laser Powder-bed-fusion processes (LPBF/M) as characterized by ISO-17296-2 [1] enable the processing of various metals, such as stainless and hot-work steel [2, 3], Aluminum [4, 5], Titanium [6] and Ni-based materials [7, 8]. Consequently, additively manufactured parts can be used in various industrial applications, such as in the tooling industry [9], lightweight engineering in automotive and aerospace 10], or components for the energy sector such as turbine blades and injection nozzles, next to applications in medical engineering like implants or instruments [10].

However, additive manufacturing technologies such as LPBF-M are still on the threshold to widespread industrial adoption, since the process characteristics limit a fast and cost-efficient qualification of the respective processes, and the corresponding parts. This is related to the fact that AM processes are categorized as master forming technologies where not only the components are manufactured, but also the incorporated material and part properties are generated in-situ with the manufacturing processes. Typically, LPBF-processed materials contain some remaining porosity, including gas porosity, next to other types of defects such as lack-of fusion or even cracks, as described by Brennan et al. [11]. Thereby, material and part properties depend on various input parameters along the process chain, including the powder properties [12-15], the main process parameters [16], build job planning including part orientation and positioning [17, 18] as-well as the readiness of quality relevant machine components, as described by Wegener and Spierings et al. [19].

For these reasons it is important to develop and implement a comprehensive quality management system along the AM process chain [19]. Such a system needs to be able to in-line acquire information about the material integrity of the processed components. McCann et al. [20] and Wegener et al. [19] provide an overview on the various monitoring technologies that are being investigated in this context. For example, Krauss et al. [21] developed a continuously monitoring system with an off-axis bolometer and a thermal detector to acquire the thermal signature of each layer and to compute a digital twin of the parts produced. Thereby, a simulated thermal diffusivity model serves to gather information about the process stability and the resulting part quality. Furthermore, various melt-pool monitoring technologies have been developed aiming to correlate the melt-pool properties and material integrity of the manufactured components. For example, Clijsters et al. [22] used an optical melt-pool monitoring system and developed routines to generate interpretable process images to estimate the quality of the part. On the other hand, Aminzadeh et al. [23] integrated as a layer-by-layer working system using a high resolution camera to image the scanned part cross-sections to assess the layer quality, and to detect top-layer porosity using a Bayesian classifier. However, defects in the top layer might be re-molten during the processing of subsequent layers, and do not necessarily remain in the components. Rieder et al. [24] demonstrated the feasibility of an ultrasonic probe mounted underneath the build platform to online monitor the AM processes through the build-platform by correlating the signals obtained with porosity generated by process instabilities. The capabilities of this approach however might be limited especially

for the production of complex shaped or fine structures. Furthermore, no information no local, real porosity can be achieved.
Common to most of the existing technologies used for material integrity assessment is the fact that material defects are detected only in an indirect way, by correlating for instance a thermal signature with certain defect types, for which machine learning methods can provide the appropriate computational methods. However, there remains a need for an in-line monitoring technology that provides direct information about the existence of local porosity of a material being processed.
Eddy current testing (ECT) is a standardized non-destructive testing technology as described by ISO-15549 [25]. It is a widely accepted quality inspection technology in industry, for instance to control and certify the quality of electrically conductive parts such as the integrity of metal structures, or turbine components. Thereby, ECT can detect material defect at the surface, or in close proximity to the surface of the components, like pores or cracks as reported by García-Martín [26]. By this, ECT seems to be a promising material integrity monitoring technology also for LPBF processes.
In this study, the suitability of the ECT for material porosity detection is demonstrated. For this purpose, LPBF manufactured specimens are scanned by ECT on a laboratory setup, and the ECT signals are correlated with relative material density. As an outlook, the integration of an ECT system into a commercial LPBF machine is demonstrated. The results underline that ECT is able to provide direct information on local material porosity, and that the proposed monitoring setup does not affect the process productivity. ECT is therefore well suited for industrial AM part quality monitoring.

2. Materials and Methods

2.1. Sample manufacturing

10 cubic SS316L samples with a size of 25 x 30 x 10 mm^3 were manufactured using a Concept Laser M2 machine operated at a Nd-YAG laser power P = 180W and with a laser spot size of 105 μm. Each sample was processed with a the same layer thickness t_L = 30 μm and hatch distance d = 100 μm, but with different scan speeds v_s = 650, 750, 850, 950, 1000, 1050, 1150, 1250, 1500 and 2000 mms^{-1} to obtain samples at density levels between ≈ 90% and 99.5%. The relative densities of the samples were measured using the Archimedes method as described by Spierings et al. [27].

2.2. Eddy current testing

The samples were EC measured in a laboratory setup allowing a x-y raster scan over the sample area (Figure 1). Linear encoders with a resolution of 0.1 mm were mounted on the axis to map sensor signals and the respective position during the raster scan area, using a pitch of 0.5mm. An eddy current instrument (UPEC Sensima Inspection) connected to a ferrite rod coil sensor with a diameter of 3mm (L = 47 μH) was used. The sensor was operated in bridge configuration at a frequency f = 200 kHz, and the coil impedance was monitored in absolute mode as described by Bowler [28].

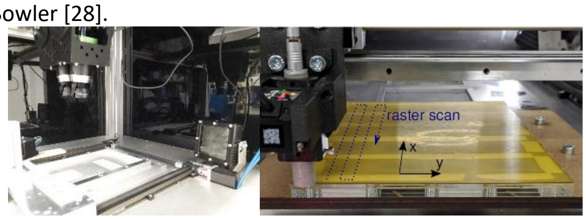

Figure 1. Left: Laboratory test bench. Right: ECT probe mounted on the recoater axis and test samples under an interlayer of 0.5 mm thickness.

Together with the electrical conductivity σ = 1.38 MSm^{-1} and magnetic permeability μ = 1.02, the standard penetration depth δ is calculated according to equation 1 [26].

$$\delta = \frac{1}{\sqrt{\pi \, f \, \sigma \, \mu_0 \, \mu_r}} \quad (1)$$

3. Results and discussion

3.1. Material density

Fehler! Verweisquelle konnte nicht gefunden werden. shows the material density for the 10 SS316L cubes, displaying a processing window range. The material defects are caused by lack of fusion and keyhole formation [11].

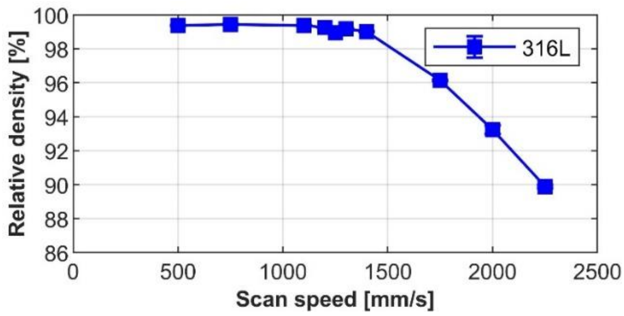

Figure 2. Relative Density of LPBF-manufactured SS316L samples

The Archimedes density, as used for Figure 2, provides only a mean density value over the entire sample volume. This assumption for homogeneously distributed pores over the sample volume is also used for industrial component production where the relative material density is not actively controlled, but the processing window is selected based on statistically validated experiments prior and in parallel to production.

3.2. Eddy current testing

Figure 3 shows the results of the ECT raster scans over the samples. Small variances in the EC sensor signals are observed in Figure 3. This indicates a high sensitivity of the ECT system to local density variations within the samples.

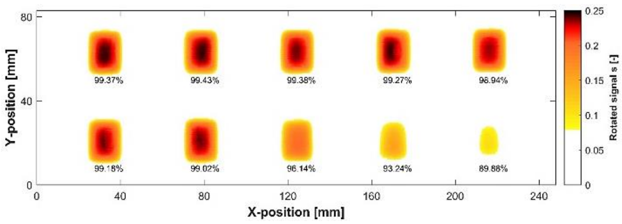

Figure 3. ECT scanning heatmap for the 10 SS316L samples

The samples were only measured by ECT on the top surface. Considering the coil diameter of 3 mm, a penetration depth of the eddy currents δ = 945 μm and a layer thickness of t_L = 30 μm, it is clear that the ECT signals provide information on the sample porosity over a comparably large local measurement volume. Hence, the current sensor design is mainly suitable for local porosity monitoring, rather than providing information on individual small defects.

Figure 3 also shows an edge effect in the signals, since towards the edge of a sample the eddy currents have to flow differently compared to the situation in the middle of a part. Therefore, only EC sensor signals from the inner region of the parts were used for further analysis. This edge effect could be further minimized by a miniaturization of the EC probe.

Figure 4 shows the correlation between the Archimedes material density measured over the cube samples, and the EC sensor signal. A very high correlation coefficient r^2 = 0.997

underlines the suitability of EC sensing for a local density measurement. Even small differences in the relative density in the range of 0.05% can be statistically distinguished, as reported by Spurek et al. [29].

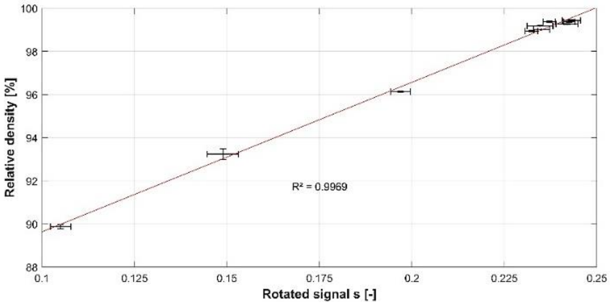

Figure 4. Correlation of relative material density and ECT sensor signal

3.3. Machine integration

To enable in-process part density monitoring the integration of an ECT system into any PBF-LB/M machine is required. Figure 5 shows a further integrated ECT system ("AMIquam") mounted on the recoater of a commercial machine, with two sensors to be placed at the positions of interest along the y-axis of the recoater. The collected data are sent to an acquisition computer outside of the machine via a wireless communication protocol, to facilitate the machine integratability.

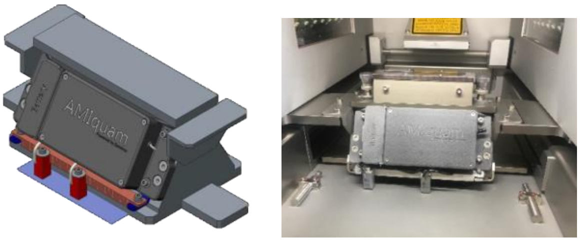

Figure 5. EC scanning system with 2 EC sensors integrated in a commercial LPBF system.

Fehler! Verweisquelle konnte nicht gefunden werden. shows a build job on the aforementioned commercial LPBF machine with four cubic samples that were ECT scanned. The build process was interrupted at certain layers, and then continued.

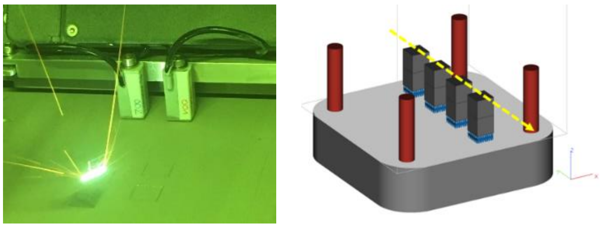

Figure 6. Left: Build process on the commercial PBF-LB/M machine with instrumented AMIquam ECT system. Right: Respective build job design.

Figure 7 shows the ECT signals as acquired over all layers of the 4 parts from the build job shown in Figure 6.

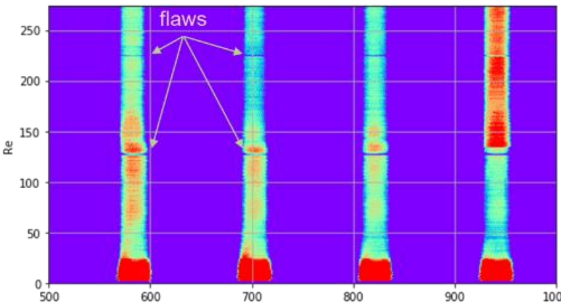

Figure 7. Image of the x-z plane of the parts obtained by ECT.

The indicated flaws represent density variations resulting from process interruptions. The layerwise monitoring of selected sections of interest within a part enables the direct generation of a digital twin of the parts by providing detailed information on real local part density.

4. Conclusions

The measured part of the ECT signal is mainly dependent on electrical conductivity σ of the material. The high coefficient of determination between relative material density ρ and electrical conductivity σ demonstrates the general suitability of the ECT technology to provide information about local porosity in the material. Hence, ECT is suitable for providing a direct path to an in-line part integrity monitoring solution for LPBF processes.

Furthermore, the statistical process control (SPC) on ECT data supports the assessment of the process window stability, and the identification of trends. Such trends in the ECT signals could be related to a drift in the condition of specific machine components, such as the cleanliness of optical components along the laser beam path, the filter system, or a drift in the laser power. A deeper integration of ECT monitoring into the control of a LPBF process and machine will further enable closed feedback loops to control processing windows to adopt for influences e.g. from changing powder properties.

The important advantages of the proposed ECT system are manifold:

- It is a cost efficient monitoring solution when compared e.g. to melt-pool monitoring
- It is an industrially widely adopted NDT technology, which can be easily integrated into commercial LPBF systems without requiring a deeper access to the machine control.
- There is no impact on LPBF process productivity.

Hence, in-process ECT monitoring can support various aspects of process monitoring and control in LPBF. It is therefore considered as an important element in a LPBF quality management system as suggested by Wegener and Spierings [19]. By that ECT is considered as an important solution to simplify process qualification and component certification and thereby to reduce related costs.

References

1. ISO-17296-2, 2020. p. 8.
2. Averyanova, M. and P. Bertrand. in *Int. Conference on Advanced Research in Virtual and Rapid Prototyping*. 2010. Leiria, Portugal: CRC Press / Balkema.
3. Spierings, A.B., et al. in *Virtual and Rapid Manufacturing: Advanced Research in Virtual and Rapid Prototyping*. 2011. Leira, Portugal: CRC Press, Taylor & Francis, London.
4. Berkau, A. in *16. Anwenderforum Rapid Product Development*. 2011. Stuttgart: citim GmbH.
5. Buchbinder, D., et al., 2014, Journal of Laser Applications, **26**(1).
6. Murr, L.E., et al., 2009, Journal of the Mechanical Behavior of Biomedical Materials, **2**(1): p. 20-32.
7. Rickenbacher, L., et al., 2013, Rapid Prototyping Journal, **19**(4): p. 282 - 290.
8. Mumtaz, K.A. and N. Hopkinson, 2009, Rapid Prototyping Journal, **15**(2): p. 96-103.
9. Reggiani, B. and L. Donati, 2018, in *Light Metal Age*. South San Francisco, CA. p. 10-17.
10. Suresh, G., K.L. Narayana, and M.K. Mallik, 2017, Additive Manufacturing, **9**(14): p. 745-755.

11. Brennan, M.C., J.S. Keist, and T.A. Palmer, 2021, Journal of Materials Engineering and Performance, **30**(7): p. 4808-4818.
12. Brika, S.E., et al., 2020, Additive Manufacturing, **31**: p. 100929.
13. Riener, K., et al., 2020, Additive Manufacturing, **101286**.
14. Spurek, M.A., et al., 2020, Additive Manufacturing, **submitted**.
15. Haferkamp, L., et al., 2021, Metals **11**(418): p. 14.
16. Delgado, J., J. Ciurana, and C.A. Rodríguez, 2012, The International Journal of Advanced Manufacturing Technology, **60**(5): p. 601-610.
17. Robinson, J., et al., 2018, Additive Manufacturing, **23**: p. 13-24.
18. Druzgalski, C.L., et al., 2020, Additive Manufacturing, **34**: p. 101169.
19. Wegener, K., et al., 2021, CIRP Journal of Manufacturing Science and Technology.
20. McCann, R., et al., 2021, Additive Manufacturing: p. 102058.
21. Krauss, H., T. Zeugner, and M.F. Zaeh, 2014, Physics Procedia, **56**: p. 64-71.
22. Clijsters, S., et al., 2014, The International Journal of Advanced Manufacturing Technology, **75**(5): p. 1089-1101.
23. Aminzadeh, M. and T.R. Kurfess, 2019, Journal of Intelligent Manufacturing, **30**(6): p. 2505-2523.
24. Rieder, H., et al., 2016, in *World Conference on Non-Destructive Testing 2016*. Munic, Germany. p. 130002.
25. ISO-15549, 2019, in *Non-destructive testing - Eddy current testing - General principles*. International Organization for Standardization (ISO).
26. García-Martín, J., J. Gómez-Gil, and E. Vázquez-Sánchez, 2011, Sensors (Basel), **11**(3): p. 2525-65.
27. Spierings, A.B. and G. Levy. in *Proceedings of the Annual International Solid Freeform Fabrication Symposium*. 2009. Austin, Texas.
28. Bowler, N., 2019, 1 ed. Springer Series in Measurement Science and Technology. New York: Springer-Verlag.
29. Spurek, M.A., et al., 2021, Metals, **submitted**.